J Mater Sci (2011) 46:3241–3251
DOI 10.1007/s10853-010-5210-0

Preparation and characterization of adipic acid-modified starch microparticles/plasticized starch composite films reinforced by lignin

Iuliana Spiridon · Carmen-Alice Teaca · Ruxanda Bodirlau

Received: 24 August 2010 / Accepted: 18 December 2010 / Published online: 30 December 2010

Abstract In this article, starch microparticles (SM) were prepared by delivering ethanol as the precipitant into starch paste solution dropwise. Adipic acid (AA)-modified starch microparticles (AASM) were fabricated using the dry preparation technique. The composites were prepared using AASM as the filler in glycerol plasticized-corn starch (GCS) matrix by the casting process. Two lignins were also compared in terms of structure and reactivity when incorporated within the AASM–GCS matrix. The effects of lignin on the morphology, surface properties, and water sorption, as well as mechanical and thermal properties of starch–lignin composite films were investigated. The surface water resistance and the thermal stability of materials were improved through addition of lignin. Starch–lignin composite materials presented higher tensile strength, but a lower elongation capacity comparatively with those without lignin.

Introduction

The great majority of plastic materials in use today are based on fossil raw materials and sustainable development in the future is expected to increase the use of renewable materials. That is why the attention for the materials based on the biopolymers has increased in the last year due to the potential replacements for synthetic composite materials in food packaging applications as a result of a strong marketing trend toward more environmentally friendly materials. Packaging composite materials made of natural biopolymers are particularly interesting due to their biodegradability, since most of these products have a relative short service life.

Great progress has been achieved in the development of biodegradable products based on polysaccharides such as cellulose, chitin, and starch, which are widely available in nature and constitute an important class of biopolymers. Among them, starch is a renewable carbohydrate polymer procurable at low cost from a great variety of crops [1, 2]. The largest source of starch is corn and the other commonly used sources are wheat, potato, and rice. Generally, corn starch consists of 20–30% amylose and 70–80% amylopectin. The hydrophilic property of these polymers is responsible for their incompatibility with most hydrophobic polymers. The interference between polymers and starch can play a critical role in obtaining composite materials with good final properties.

The starch-based materials can be attractive for different market segments such as food packaging and mulch foils and plant pots (horticulture/landscape). Also, this biopolymer is susceptible to versatile physical and chemical modifications [3, 4]. Unfortunately, the hydrophilic nature of starch which makes it dependent on the ambient humidity limits the applications of this biopolymer. As a consequence, native starches are often chemically modified to improve the product properties and thus to enhance their application range [5–7]. For food applications, chemical modifications lead to products with improved texture, quality, shelf life, and improved processing tolerance, such as improved heat, shear, and acid stability [5]. Modified starches are used as thickeners, gelling, and encapsulating agents in the food sector [8]. Chemical modification also

I. Spiridon · C.-A. Teaca (✉) · R. Bodirlau
Department of Natural Polymers, "Petru Poni" Institute of Macromolecular Chemistry, 41A Grigore Ghica-Voda Alley, Iasi 700487, Romania
e-mail: cateaca14@yahoo.com

allows starches to be employed in the non-food industry. Examples may be found in the paper industry where modified starches are used as wet-end additives, sizing agents, coating binders, and adhesives. Modified starches are also used as textile sizes and in tableting and cosmetic formulations [5, 8]. Well-known chemical modification reactions are esterification, etherification, and cross-linking [9].

Cross-linking is a common approach to improve the performance of starch for various applications. Cross-linking reagents may be any chemical containing two or more functional groups capable of reacting with at least two of the hydroxyl groups on the starch molecule and thus causing a linkage of those groups. The most widely used cross-linking reagents for modifying food starches are mixtures of adipic/acetic anhydride, and phosphorus oxychloride or sodium trimetaphosphate, which yield distarch adipates, distarch phosphates, respectively [6, 10]. Adipic acid (AA) reacts with starch and produces both cross-linked starches and monoderivatives. Some advantages of cross-linked starches over native starches are: increased stability toward heat, pH, shear, and freeze–thaw stability [11, 12].

One significant approach is the use of inorganic or organic reinforcement to prepare starch-based nanocomposites, which can be obtained by filling plasticized starch matrix with nanofillers such as layer silicates [13, 14], carbon nanotubes [15], carbon black (CB) [16], cellulose [17], and starch nanoparticles [18, 19].

Delignification processes employed by the pulp and paper industry yield abundant and renewable by-products referred to as industrial alkaline lignins, being abundant and low-cost materials. These lignins can be advantageously used in biomass conversion processes for biofuel production [20] or as fillers in natural thermoplastics such as starch [21, 22], cellulose derivatives [23], proteins [24, 25], or polyesters [26].

In this article, starch microparticles (SM) were prepared using a commercially corn starch, being further modified by reaction with AA to obtain modified starch microparticles (AASM) by the dry preparation technique. The starch composites were prepared using AASM as the filler in glycerol plasticized-corn starch (GCS) matrix by the casting process. Subsequently, two lignin samples (one separated from beech wood, one industrial kraft lignin extracted by precipitation in the Ligno-Boost process) were incorporated within the AASM–GCS matrix as filler. Changes in the starch and composite materials structure were studied through X-ray diffraction (XRD) and FTIR spectroscopy. The effects of lignin were investigated through mechanical tests, wettability, and water sorption tests, as well as optical and thermal properties of starch–lignin composite materials.

Experimental

Materials

A commercially corn starch (S) constituted the continuous matrix of the composite films. Amylose and amylopectin contents were 25.3 and 74.8%, respectively, while residual protein (gluten) was less than 0.3%. Glycerol was purchased from Fluka (98% purity, Fluka Chemical, Germany) and used as plasticizer. The beech lignin was separated from beech wood by Tappi method and Boost lignin was supplied by the Sodra Company (Sweden). Reagents as ethylene glycol and AA were provided by Chemical Company, Iasi, Romania.

Preparation of SM and AASM

10 g S was added into 200 mL of distilled water. The mixture was heated at 90 °C for 1 h for the complete gelatinization of corn starch with constant stirring, and then 200 mL of ethanol was added dropwise to the solution of gelatinized starch solution with constant and vigorous stirring. When the resulting SM suspensions were cooled at the room temperature, another 200 mL of ethanol was added dropwise for about 50 min with constant stirring. The suspensions were centrifuged at 8000 rpm for 20 min, and the settled SM was washed using ethanol to remove the water. After complete washing, the SM was dried at 50 °C to remove ethanol.

The AA (20 g) was dissolved in 100 mL of ethanol. SM (3.5 g) was mixed with 15 mL of adipic acid solution in a glass tray and conditioned for 12 h at room temperature to allow the absorption of adipic acid solution by SM. The tray was dried in vacuum at about 2 mmHg and 50 °C for 6 h to remove ethanol. The obtained mixture was ground and dried in a forced air oven for 1.5 h at 130 °C. The dry mixture was washed three times with water to remove non-reacted AA. AASM mixtures were finally washed with ethanol to remove water, dried at room temperature, and ground. The dried SM and AASM were used for obtainment of composite films with Boost lignin and beech lignin, respectively. Compared to starch nanocrystals [27], AASM is not gelatinized during the processing of the composites. It can be used as a reinforcing agent for glycerol-plasticized starch.

Preparation of AASM/S/lignin composite material

The AASM particles were dispersed in a solution of distilled water (100 mL) and glycerol (1.5 g) for 1 h before adding 5 g corn starch and 0.2 g lignin (beech lignin-coded as BeL, Boost lignin-coded as BoL). AASM and lignin filler loading level (4 wt%) was based on the amount of

starch. The mixture was heated at 90 °C for 0.5 h with constant stirring to plasticize the corn starch. To obtain the AASM/S/lignin composite films, the mixture was cast using a fast coating technique namely the doctor blade technique. Films were obtained by dropping and spreading the mixture on a glass plate using a blade with a slit width of 0.8 mm. After degassing in a vacuum oven at 50 °C for 24 h up to constant weight, the films were air cooled and detached from the glass surface to be investigated. Films with a thickness of ~0.2 mm were obtained, this value resulting from measurements by means of a digital micrometer. The composite materials, coded as AASM/S/BeL and AASM/S/BoL, were preconditioned in a climate chamber at 25 °C and 50% RH for at least 48 h before the testing. Water content of the composite films was around 9 wt%.

XRD

The crystalline structure of the S, SM, and AASM was studied by XRD using a Bruker AD8 ADVANCE X-ray diffractometer with CuKα radiation at 60 kV and 50 mA, at room temperature. Scattered radiation was detected in the diffraction angle 2θ ranging from 10 to 30° at a rate of 2° min^{-1}.

Fourier Transform Infrared (FTIR) spectroscopy

The FTIR spectra of composite materials were recorded on a Bruker Vertex 70 spectrophotometer. The spectral resolution was 4 cm^{-1} and the scanning range varied from 400 to 4000 cm^{-1}.

Polarized light microscopy

Sample surface of the composite materials was observed using a LEICA-DMLP light microscope after 1 week storage at 25 °C and 50% relative humidity (RH) with no further preparation. Images (magnification 10×) were collected with a CCD camera.

Scanning electron microscopy (SEM)

The SM/S, AASM/S, AASM/S/BoL, and AASM/S/BeL films were investigated using a SEM (FEI QUANTA 200ESEM). Air dried samples were fixed onto aluminum stubs through carbon adhesive disks and their surface was observed with a low-vacuum secondary electron detector using the accelerating voltage of 25.0 kV. The samples were analyzed at room temperature and at an internal pressure of 0.50 torr.

Film opacity

The composite materials opacity was measured by a JENWAY 6405 UV–Vis spectrophotometer and defined as the area under the absorbance spectrum between 400 and 800 nm according to the ASTM D 1003-00 method (ASTM D 1003-00 Standard Test Method for Haze and Luminous Transmittance of Transparent Plastics). The film samples were cut into a rectangular piece (1 × 2.5 cm, 0.2 mm thickness), fixed on the inner side of a 1-cm spectrophotometer cell and the absorbance spectrum recorded. The film opacity determinations were repeated three times.

Particle size analysis

Particle size analysis was carried out by using a laser diffractometer (Mastersizer 2000, Malvern Instruments). The samples were diluted in water (concentration of 0.05%) at 2000 rpm until an obscuration rate of 12.06% was obtained. Three samples were measured in quintuplicate. The Mie theory was applied by considering the following optical properties: RI for starch of 1.527 and absorption of 0.001.

Contact angle measurements

The films were kept 48 h at 50% RH before being tested in static conditions on a KSV CAM 200 goniometer. A 2.5 μL droplet of water was applied on the film surface. The evolution of the droplet shape was recorded every second by a video camera and image analysis software was used to determine the contact angle. Water and ethylene glycol were employed as liquids with different polarity. The value reported is the average of ten measurements.

Water uptake of the composite films

To determine the water absorption [28], the composite materials specimens used were thin rectangular strips with dimensions of 10 × 10 × 0.2 mm. The films were supposed to be thin enough so that the molecular diffusion was considered to be one-dimensional and were vacuum-dried at 90 °C overnight. After weighing, they were conditioned at 25 °C in a desiccator containing sodium sulfate to ensure a RH of 95%. They were then removed at specific intervals and gently blotted with tissue paper to remove the excess of water on the surface, and the water uptake was calculated with Eq. 1, as follows:

$$\text{Water uptake}(\%) = [(W_t - W_0)/W_0] \times 100, \quad (1)$$

where W_t and W_0 represents the weight at time t and before exposure to 95% RH, respectively. The determinations were performed in triplicate.

Mechanical properties of the composite films

Tensile stress and strain at break were evaluated according to ASTM D882-00 (ASTM D882-00 Standard Test Method for Tensile Properties of Thin Plastic Sheeting) using an Instron 3345 with a 5-kN load cell. Before testing, the films were cut into strips and conditioned at 50% RH and 25 °C for 1 week. Testing was done on samples each measuring 10 × 1 cm randomly cut from the cast films. The thickness of each specimen was measured at four points along its length with digital micrometer. The crosshead speed was 10 mm min^{-1}. A minimum of ten replications of each test sample were run.

Thermal analysis

The TG/DTG analysis was performed using a Netzsch STA 449 F1 Jupiter system under nitrogen atmosphere. The measurements were performed while heating the samples (≈5 mg) placed in Al_2O_3 crucibles hermetically closed with lids at a rate of 10 °C min^{-1} from room temperature up to 600 °C and using nitrogen as a purging gas at a flow rate of 50 mL min^{-1}. TG curves recorded with a ±0.5 °C precision were analyzed using a Netzsch Proteus analysis software.

Results and discussion

XRD

The native corn starch generally presents sharp diffraction peaks at 15.3°, 17.5°, and 23.1° (2θ). SM and AA-modified starch showed a similar native profile, but AASM presented a new peak at ~22.5° (2θ) which appeared as diffusion peak of adipated starch. The XRD indicated that during starch modification process, several crystalline structures of native starch were destroyed, and a new structure of adipated starch was formed (Fig. 1).

The diffraction peaks of native corn starch decreased in intensity by addition of AA. The diffraction peaks for SM and AASM look like a V-type starch structure, which is different from A-type diffraction pattern in corn starch, as it is shown in Fig. 1. This could be due to the single helical structure "inclusion complex" made up of amylose and plasticizer [29]. The similar V-style crystallinity also appeared in the plasticized corn starch [15]. The gelatinization destroyed A-style crystallinity of corn starch, and

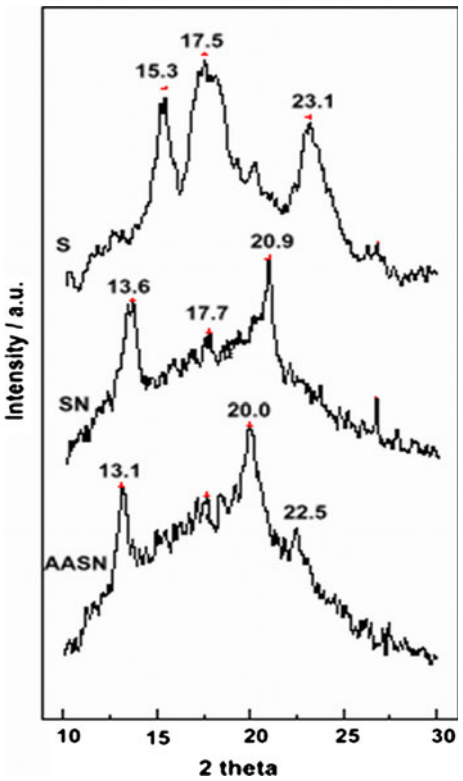

Fig. 1 XRD diffractograms recorded for S, SM, and AASM powders

SM exhibited the V-style crystallinity. When AA penetrated the SM granule, it could disrupt to a less extent the V-style crystalline structure of starch, the reaction occurring both in the amorphous and crystalline phase [30]. Substitution of AA groups on starch chains could form a highly cross-linked starch and thus limit starch chain mobility.

FTIR spectroscopy

The FTIR spectroscopy was employed to investigate the interactions between starch and lignin in composite materials. The infrared spectra of the components and composite films are presented in Fig. 2a, b.

Figure 2a showed the FTIR spectra of S, SM, and AASM powders, as well as the spectra recorded for BeL and BoL. Corn starch and SM exhibited similar FTIR spectra. It can be observed that several noticeable changes occur in the spectra of SM and AASM. The characteristic peak occurred at 1650 cm^{-1}, which Fang et al. [31] believed to be a feature of tightly bound water present in the starch. The absorption bands between 1000 and 1200 cm^{-1} were characteristic of the –C–O– stretching on polysaccharide skeleton.

The neat starch and starch composite films present similar features in the two FTIR spectral regions, with the

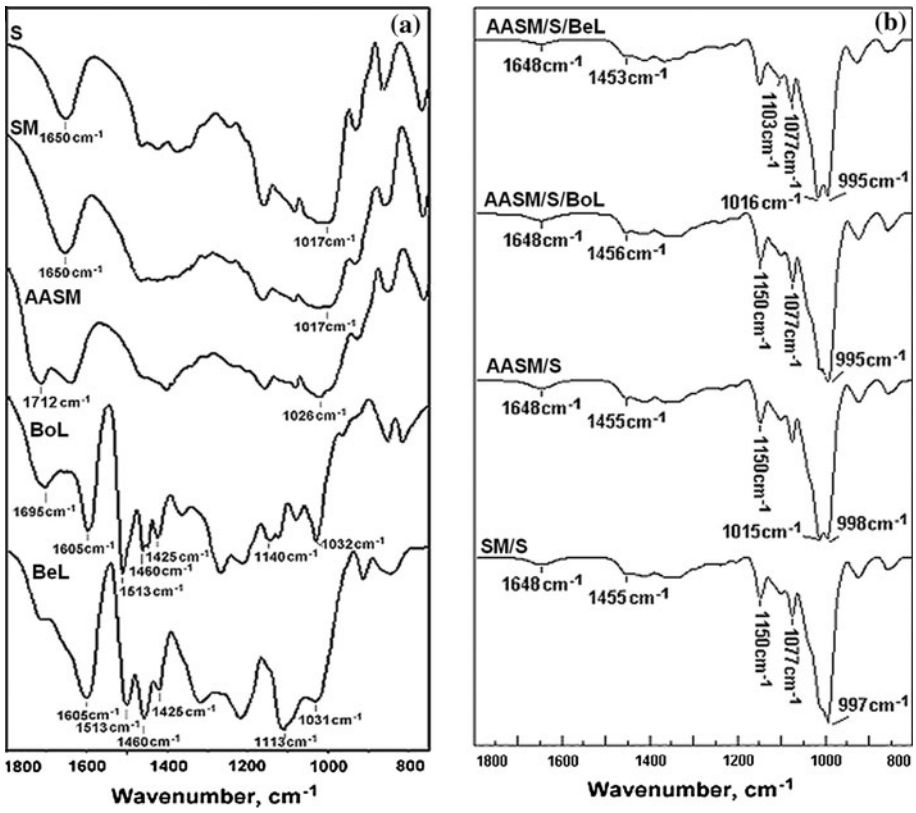

Fig. 2 FTIR spectra recorded for the S, SM, AASM, BoL. BeL (**a**) and SM/S, AASM/S, AASM/S/BoL, and AASM/S/BeL films (**b**)

exception of the peaks related to the absorptions of the hydroxyl groups, at 1650 and 1017 cm^{-1}. As it can be seen, the band at high wave number show a very slight broadening with the incorporation of SM, while the band at 1017 cm^{-1}, associated with the C–OH bond, show significant changes in the relative intensity of the doublet in agreement with the report of Van Soest et al. [32]. The slight broadening of the peaks, associated with OH groups, suggests an increase in the number of oscillation modes, which could be associated with the presence of different types of hydrogen bonding interactions.

For AASM powders, a new peak occurred at 1712 cm^{-1} is assigned to C=O stretching vibration [33]. The presence of the carbonyl peak indicates that SM were successfully reacted with AA. In S and SM, the oxygen of the C–O–C group could form the hydrogen-bond interaction with the hydrogen of hydroxyl groups, while the ester bonds in AASM as the cross-linking of starch sterically hindered this hydrogen-bond interaction. According to Huang et al. [34] the weakening of this interaction made C–O bond stretching of the C–O–C group shifted to 1026 cm^{-1}.

The two kinds of lignin (BeL and BoL) have different FTIR spectra, typical of hardwood and softwood lignins, respectively [35]. A close examination reveals significant differences in some areas which are outlined in Fig. 2a. The BoL spectrum is evidenced by a strong band between 1650 and 1750 cm^{-1} with a maximum at 1695 cm^{-1} corresponding to conjugated carbonyl stretching. This band is less pronounced in the spectrum of BeL. This result suggests higher carbonyl content in BoL, in agreement with Pandey [35]. Between 1200 and 800 cm^{-1}, the spectra differ in the resolution between the two bands at 1150 and 1120 cm^{-1}, corresponding to aromatic C–H in-plane deformation and to C–O and C–C stretching of the carbohydrates associated to lignin.

Chemically, softwood lignins consist largely of guaiacylpropane units, while hardwood lignins are made up of both guaiacylpropane and syringylpropane units. Both lignins contain predominately glycerol–aryl ether linkages, but there are several types of C–C bonds which likely serve as cross-links between relatively short, linear chains of phenylpropane units. Softwood lignins contain fewer glycerol–aryl ether linkages and subsequently a more complex macromolecular network structure. It is apparent from Fig. 2a that the characteristic bands of lignin at 1605, 1513, 1460, and 1425 cm^{-1} correspond to aromatic ring vibration of the phenylpropane skeleton. The peaks at 1140 and 1113 cm^{-1} evidence the presence of guaiacyl C–H in BoL and syringyl C–H in BeL, respectively [35].

Figure 2b shows the FTIR spectra of SM/S, AASM/S, and AASM/S/lignin (BeL and BoL) films. Through addition of glycerol, new hydrogen bonds are formed. The bands at 1648 and 1455 cm^{-1} were assigned to the O–H bending of water and CH_2, respectively. The bands at 1150

and 1077 cm^{-1} were attributed to the stretching vibration of C–O in C–O–H groups, and the band at 1016 cm^{-1} was attributed to the stretching vibration of C–O in C–O–C groups. All peaks shifted to a lower wave number than those of starch. This indicated that new hydrogen bonds were formed between components in the composite films. The band located at 1080 cm^{-1} (in S, SM, and AASM) for C–O stretching is shifted to 1077 cm^{-1} in the AASM/S/lignin composite films. The absorption band located at 997 cm^{-1} in SM/S and 998 cm^{-1} in AASM/S (assigned to C–O bond stretching of C–O–C group in the anhydroglucose ring of the starch) is shifted to 995 cm^{-1} in AASM/S/BoL and AASM/S/BeL, respectively. The strong peaks observed at 995, 1016, and 1077 cm^{-1} are specific to the anhydroglucose ring in starch, although these signals could also be associated with the presence of glycerol molecules.

All the changes in wave number indicate obvious interactions among the hydroxyl, carbonyl, and ether groups of the starch and lignin components. These changes can be attributed to the hydrogen bonding possibly occurred between hydroxyl, carbonyl groups in starch and carbonyl, hydroxyl, ether groups in lignin.

Film morphology

Optical micrographs of the both starch and starch/lignin composite films are shown in Fig. 3.

The first two micrographs of SM/S (a) and AASM/S films (b) are smooth and are significantly different from that of the starch/lignin films (c, d) which have some discontinuousness, related to distribution of lignin particles. Morphologically, the starch-based films exhibit a two phase structure, in which lignin particles are dispersed within a continuous phase of thermoplastic starch. The low casting temperature can be responsible for the amorphous structure.

SEM

The SEM technique was used to establish the lignin filler dispersion within the final composite films. Figure 4 shows SEM micrographs that were obtained for the corn starch (a, b), and film samples including SM/S (c), AASM/S (d), and those comprising lignin fillers, AASM/S/BoL (e), and AASM/S/BeL (f).

In the processing of SM, native granular corn starch (Fig. 4a) was gelatinized in water and formed starch paste. The preparation of starch in water by dropwise addition of ethanol resulted in the SM (Fig. 4c). The reaction of SM and AA seemed to decrease the aggregation of SM and large particles of SM reduced in Fig. 4d.

As shown in Fig. 4d, no residual granular structure of corn starch was observed in the continuous GCS phase. At the high temperature, water and glycerol were known to physically break up the granules of corn starch and disrupt intermolecular and intramolecular hydrogen bonds and make the native starch plastic. However, AASM was not destroyed, because the substitution of AA groups cross-linked starch. AASM was dispersed well in the plasticized starch matrix without obvious aggregation. Substitution of AA groups on starch chains could form a cross-linked starch, limit starch chain mobility and thus ensure the

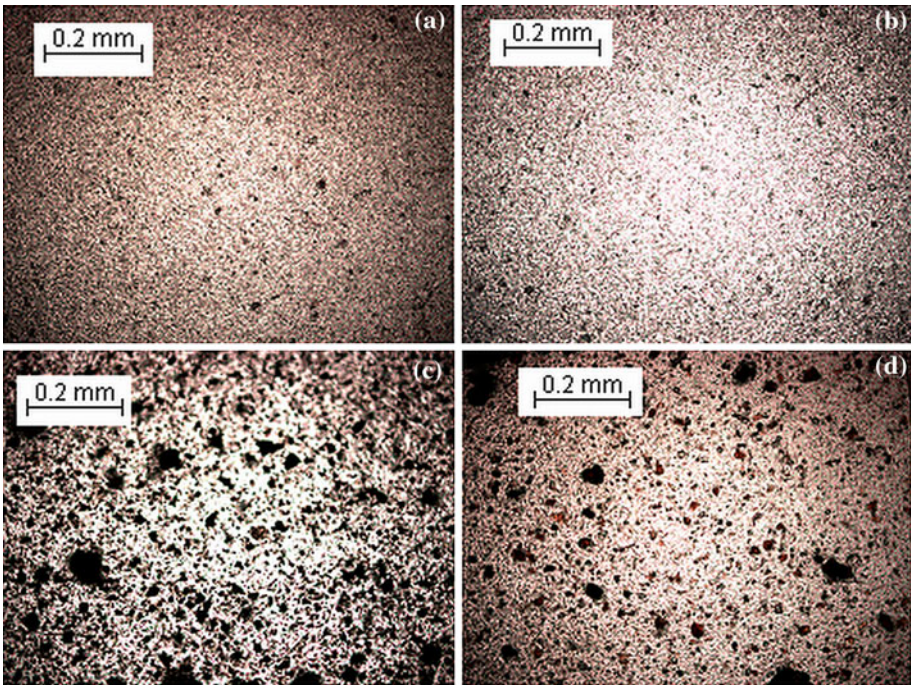

Fig. 3 Micrographs of the different starch films: **a** SM/S; **b** AASM/S; **c** AASM/S/BoL; and **d** AASM/S/BeL

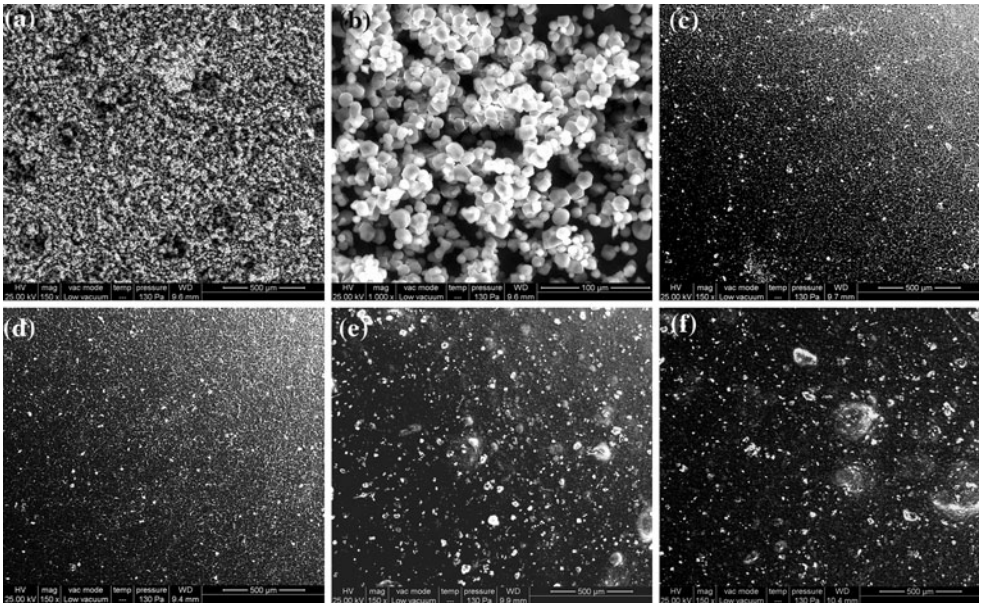

Fig. 4 SEM micrographs from the surface analysis of: S (×150, **a**), S (×1000, **b**) powder, SM/S (×150, **c**), AASM/S (×150, **d**), AASM/S/BoL (×150, **e**), and AASM/S/BeL (×150, **f**) films

AASM as reinforcing agents in the matrix represented by the GCS.

The lignin particles seem to be better coated by the plasticized starch matrix. This effect is related to the morphology of the filler. Because lignin particles have a more uniform shape, these are easier to be coated by a softened thermoplastic, such as plasticized starch during obtaining films.

The filler particles near the surface present a strong tendency to be coated by the plasticized starch matrix. The presence of the fillers seems to increase slightly the roughness of the surface, creating a less homogeneous surface (as seen in Fig. 4e, f).

It was also seen that the dispersion of the filler exhibits a slightly particle aggregation for composite films considered. A relative good dispersion and alignment tendency of the filler within the composites is observed due to the lower loading level, the amount of thermoplastic being larger than that of the filler in weight.

Film surface properties

Opacity is a very important characteristic for the films with applications in food packaging. It provides information on the particle size of dispersed particles in starch matrix. Thus, the particle sizes larger than the visible wavelength would obstruct light, leading to opaque composite materials.

Figure 5 shows the opacity of the obtained films. Not surprisingly, lignin reduced film transparency when it was applied to film, as shown in Fig. 5, due to its chromophoric nature. On the other hand, however, it can effectively inhibit ultraviolet radiation, which is an important property for agricultural mulching, as well as other industrial applications. In fact, a few percent composition of lignin in starch films could effectively function as an ultraviolet scavenger without any significant perturbations on film water absorbency.

It seems that opacity of starch–lignin composite films depends on the lignin type, the opacity of AASM/S/BoL composite being higher than that of the AASM/S/BeL

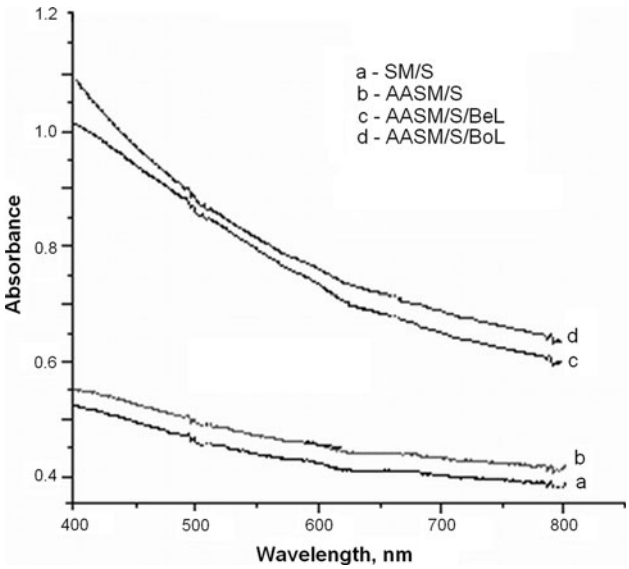

Fig. 5 Evolution of the opacity recorded for SM/S, AASM/S, AASM/S/BoL, and AASM/S/BeL composite films

composite. This can be associated with the particle size of lignin. The larger the particle size the lesser the light transmission, therefore the results of light transmittance further proved that the particle size of Boost lignin is smaller than that of beech lignin, as seen in Fig. 6.

The use of starch modified with AA causes the increase of the contact angle between the liquid droplet and the surface over which it spreads. This is because surface of film containing non-modified starch (SM/S) was more OH-rich macromolecules and has the capability to establish hydrogen bonds with liquid molecules. The presence of lignin increased the contact angle between water and ethylene glycol drop with starch–lignin composite materials surface as compared to AASM/S film (Table 1). This should not be surprising given that a hydrophobic component was added.

In a multiple biopolymer system, each biopolymer not only contributes to the film properties but also engages in biopolymer–biopolymer interactions that affect the overall system properties. Occasionally, these interactions are more important than individual actions. Chemical structure, ratio of amylose to amylopectin, polymer packaging, crystallinity, and plasticizer influence the permeability of starch films [36]. Owing to the strong hydrophilicity of starch molecules, a neat starch film displays high water absorbency. This factor impedes the application of pure starch films for most non-absorbency applications. It can be observed that the AASM/S film has absorbed less water than SM/S film. The formation of a more tight structure after cross-linking prevents the swelling of starch and also restricts the movement of molecules, leading to a decrease of the amount of adsorbed water in agreement with mechanical properties.

However, incorporation of lignin into the starch matrix was able to reduce to a lesser extent the water absorbency of AASM/S/BoL and AASM/S/BeL films as shown in Fig. 7. The hydrophobic lignin plays an important role in improving surface and bulk-hydrophobation of the starch-based materials, which prevents water from spreading or being absorbed. The water uptake-time curves exhibit two well-separated zones. At short times, below 25 h, the kinetics of absorption is very fast, whereas at long times, after 25 h, the kinetics of absorption is slow and leads to a plateau, corresponding to the equilibrium of water uptake. Therefore, the swelling of the films is reduced by incorporating lignin into the plasticized starch matrix. The improvement of surface and bulk-hydrophobation of the starch-based films, resulted from addition of lignin, cannot be negligible. The presence of lignin causes the water resistance increasing and could improve the application property of the composite films.

Table 1 Average contact angle for starch, modified starch, and starch–lignin composite films

Samples	SM/S	AASM/S	AASM/S/BoL	AASM/S/BeL
Ethylene glycol	21.7	28.73	35.2	31.23
Water	42.22	45.35	59.69	49.15

Mechanical properties

The poor strength properties (elastic modulus, tensile, and compression) of neat starch films are major drawbacks for their use in diverse commercial applications. Improvements in the mechanical properties of film are therefore mandatory.

The presence of lignin in the starch matrix could act as reinforcement filler impacting both the mechanical and physical properties of the starch/lignin composite films.

Table 2 summarizes the mechanical properties of the composite films, which were evaluated as tensile strength, Young modulus and elongation at break. The tensile strength of composite films was influenced by the components. Thus, the presence of modified starch increased the elongation at break and decreased both the Young modulus and tensile strength. By addition of lignin, the tensile strength was improved. However, as a result of more compact structure due to high intermolecular hydrogen bond between polymers, the composite materials were more brittle than the original films.

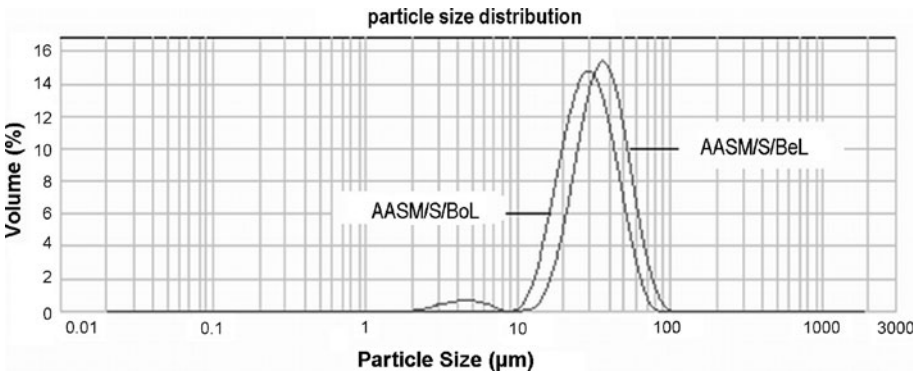

Fig. 6 Particles size distribution for AASM/S suspensions containing lignin fillers, BeL and BoL, respectively

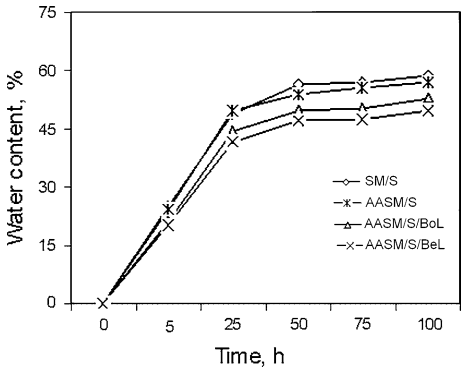

Fig. 7 Water uptake-time curves obtained for the SM/S, AASM/S, AASM/S/BoL, and AASM/S/BeL composite films

Thermal analysis

The TG/DTG investigation of the samples was performed to study their thermal decomposition behavior. TG curves obtained for starch-based composite materials (SM/S, AASM/S, AASM/S/BeL, and AASM/S/BoL) are presented in Fig. 8. The thermal decomposition process of the SM/S and AASM/S composite materials presents three main stages of reaction, which agree with previous reports [37–39]. The first stage corresponds to the loss of water, the second stage is due to the decomposition of the glycerol-rich phase, which also contains starch, and the third stage corresponds to the oxidation of the partially decomposed starch [37].

The TG thermal derivate (DTG) curves show that a wide peak appears around 100 °C, which can be associated with the maximum in the water loss rate. DTG signals evidenced the following stages: one around 200 °C, where the decomposition of the glycerol-rich phase occurs and another around 320 °C, associated with the degradation of the starch-rich phase. This result agrees with the FTIR spectroscopy results with regard to the presence of hydrogen bonding (glycerol–SM) in the composite materials. The degradation occurring around 320 °C, associated with starch degradation, is similar in all the samples.

As it can be observed, thermal decomposition of the starch–lignin composite materials can be divided into three individual stages: moisture evolution, starch decomposition,

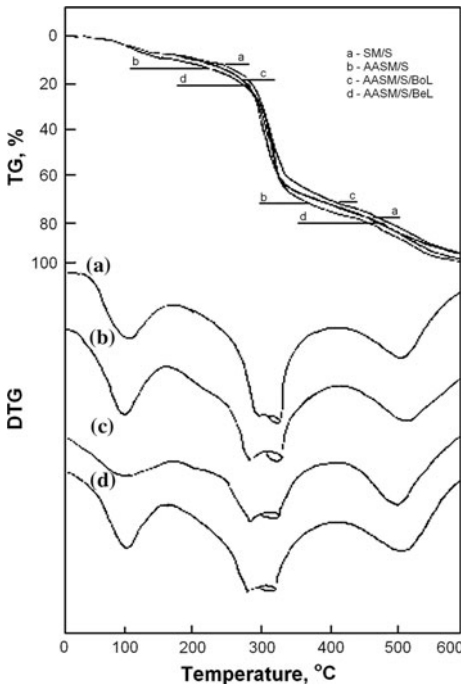

Fig. 8 TG curves recorded for the SM/S, AASM/S, AASM/S/BoL, and AASM/S/BeL composite films

and lignin decomposition. The different interactions between the molecules, as well as the cross-links formation, influenced the thermal degradation of starch–lignin composite materials. The decomposition is evidenced in a wide temperature range; the major devolatilization step occurring between 200 and 600 °C. Thus, the peak observed at 100 °C is attributed to water volatilization, while the peak at around 300 °C can be assigned to the decomposition of starch. The third peak at around 500 °C may be attributed to the lignin decomposition and the thermo-oxidative process of the partially decomposed starch. However, lignin was more difficult to decompose, as its weight loss occurred in a wide temperature range (from 160 to 900 °C) [40].

The decomposition curves of starch-based films and reinforced with lignin are partially overlapped (Fig. 8), due to the component of each film: starch, modified starch, lignin. The temperature at the maximum degradation rate,

Table 2 Mechanical properties recorded for the starch, modified starch, and starch–lignin composite films

Composite films	Young modulus (MPa)	Tensile strength (MPa)	Elongation at break (%)
SM/S	1633	22.4	4.6
AASM/S	1162	11.5	7.8
AASM/S/BoL	1074	16.9	4.8
AASM/S/BeL	796	13.9	5.5

Each value is the average of seven samples

Table 3 Temperatures for the maximum degradation rate of the starch, modified starch, and starch–lignin composite films

Samples	Temperature at the maximum degradation (°C)	Weight loss at 600 °C (%)
SM/S	325	95
AASM/S	320	98
AASM/S/BoL	315	92
AASM/S/BeL	315	95

obtained for all composite materials with different components was evidenced (Table 3).

The weight loss for the starch–lignin composite materials before the onset temperature was related to the volatilization of water and glycerol [41]. In the temperature range of 295–350 °C, the maximum decomposition was observed. At 600 °C, 92% of AASM/S/BoL composite material was decomposed, while 98% of AASM/S sample was decomposed at the same temperature. The introduction of lignin increases thermal stability, suggesting that inter-component H-bonding increased the thermal stability of the AA-modified starch/plasticized starch composite materials.

Conclusions

The incorporation of lignin within starch matrix can modify the physical and chemical properties of starch-based composite materials. Some important improvements for starch-based materials could be achieved, while maintaining the natural advantages of starch films.

In this article, starch–lignin composite materials were prepared from modified SM originating from starch previously cross-linked by reaction with AA as filler in GCS matrix by the casting process. Two kinds of lignin, one obtained at laboratory scale from beech wood and another one industrial kraft lignin, were incorporated within the polymer matrix mentioned above.

The XRD and FTIR spectroscopy evidenced the changes in the structure of starch, SM, and modified SM. The absorption peaks corresponding to the hydroxyl, carbonyl, and ether groups in starch have a tendency to shift to higher wave number for the starch–lignin composite materials, indicating the existence of a hydrogen-bonding interaction between starch and lignin. Mechanical tests, wettability, and water sorption tests, as well as optical and thermal properties of starch–lignin composite materials were investigated.

Optical microscopy evidenced a two phase structure, in which lignin particles are dispersed within a continuous phase of thermoplastic starch. Starch/lignin composite materials presented higher tensile strength and were more rigid, but had lower elongation capacity. The lignin component in the modified starch composite materials increased the thermal stability. At the same time, the obtained composite materials became more hydrophobic, a decrease of the water absorption in a high-humidity atmosphere being observed. Films transparency was also seen to decrease with addition of lignin. Our study provides a simple and cheap way to prepare fully biodegradable modified starch/lignin composite materials, which may have wide application in the packaging or agricultural mulching.

References

1. Gonzalez-Gutierrez J, Partal P, Garcia-Morales M, Gallegos C (2010) Biores Technol 101:2007
2. Angellier H, Molina-Boisseau S, Dole P, Dufresne A (2006) Biomacromolecules 7:531
3. Bonacucina G, Di Martino P, Piombetti M, Colombo A, Roversi F, Palmieri GF (2006) Int J Pharm 313:72
4. Wang LF, Pan SY, Hu H, Miao WH, Xu XY (2010) Carbohydr Polym 80:174
5. Schwartz D, Whistler RL (2009) In: BeMiller JN, Whistler R (eds) Starch: chemistry and technology, 3rd edn. Academic Press, New York
6. Wurzburg OB (1986) In: Wurzburg OB (ed) Modified starches: properties and uses. CRC Press, Boca Raton
7. Tharanathan RN (2005) Crit Rev Food Sci Nutr 45:371
8. Chiu CW, Solarek D (2009) In: BeMiller JN, Whistler R (eds) Starch: chemistry and technology, 3rd edn. Academic Press, New York
9. Huang JR, Schols HA, Klaver R, Jin ZY, Voragen AGJ (2007) Carbohydr Polym 67:542
10. Mali S, Grossmann MVE (2001) LebensmWissTechnol 34:384
11. Ellis RP, Cochrane PM, Daley MFB (1998) J Sci Food Agric 77:289
12. Reddy N, Yang Y (2010) Food Chem 118:702
13. Ma XF, Yu JG, Wang N (2007) Macromol Mater Eng 292:723
14. Almasi H, Ghanbarzadeh B, Entezami AA (2010) Int J Biol Macromol 46:1
15. Ma XF, Yu JG, Wang N (2008) Compos Sci Technol 68:268
16. Ma XF, Chang PR, Yu JG, Lu PL (2008) Starch/Stärke 60:373
17. Cao XD, Chen Y, Chang PR, Stumborg M, Huneault MA (2008) J Appl Polym Sci 109:3804
18. Garcia NL, Ribba L, Dufresne A, Aranguren MI, Goyanes S (2009) Macromol Mater Eng 294:169
19. Ma XF, Jian RJ, Chang PR, Yu JG (2008) Biomacromolecules 9:3314
20. Chakar FS, Ragauskas AJ (2004) Ind Crops Prod 20:131
21. Baumberger S, Monties B, Valle GD (1998) Polym Degrad Stab 59:273
22. Baumberger S (2002) In: Hu TQ (ed) Chemical modifications, properties, and usage of lignin. Kluwer Academic/Plenum Publishers, New-York
23. Ghosh I, Jain RK, Glasser WG (1999) J Appl Polym Sci 74:448
24. Huang J, Zhang LN, Chen FG (2003) J Appl Polym Sci 88:3284
25. Huang J, Zhang LN, Chen FG (2003) J Appl Polym Sci 88:3291
26. Li JC, He Y, Inoue Y (2003) Polym Int 52:949
27. Le Corre D, Bras J, Dufresne A (2010) Biomacromolecules 11:1139

28. Dufresne A, Vignon MR (1998) Macromolecules 31:2693
29. Van Soest JJG, Vliegenthart JFG (1997) Trends Biotechnol 15:208
30. Xie XJ, Liu Q, Cui SW (2006) Food Res Int 39:332
31. Fang JM, Fowler PA, Tomkinson J, Hill CAS (2002) Carbohydr Polym 47:245
32. Van Soest JJG, Tournois H, de Wit D, Vliegenthart JFG (1995) Carbohydr Res 279:201
33. Yang CQ, Andrews BAK (1991) J Appl Polym Sci 43:1609
34. Huang MF, Yu JG, Ma XF (2004) Polymer 45:7017
35. Pandey KK (1999) J Appl Polym Sci 71:1969
36. Chung YL, Hsi-Mei L (2007) Starch/Stärke 59:583
37. Wilhelm HM, Sierakowski MR, Souza GP, Wypych F (2003) Carbohydr Polym 52:101
38. Jiang W, Qiao J, Sun K (2006) Carbohydr Polym 65:139
39. Rath SK, Singh RP (1998) J Appl Polym Sci 70:1795
40. Yang H, Yan R, Chen H, Lee DH, Zheng C (2007) Fuel 86:1781
41. Ma XF, Yu JG, Ma YB (2005) Carbohydr Polym 60:111